ELSEVIER

Polymer 42 (2001) 3259–3270

polymer

www.elsevier.nl/locate/polymer

Characterization of the graft copolymers formed in situ in reactive blends

Hyun Kyoung Jeon[1], Hyun Taek O, Jin Kon Kim*

Department of Chemical Engineering, Polymer Research Institute (PRI), Electric and Computer Engin. Divisions, Pohang University of Science and Technology, Pohang, Kyungbuk 790-784, South Korea

Received 9 May 2000; accepted 26 June 2000

Abstract

The graft copolymers formed in situ in the 75/25 (wt/wt) mono-carboxylated polystyrene [PS-mCOOH]/poly(methyl methacrylate-*ran*-glycidyl methacrylate) [PMMA–GMA] blends depending upon the molecular weight and the number of the epoxy functional groups (f) in PMMA–GMA were characterized using proton nuclear magnetic resonance spectroscopy and gel permeation chromatography. The graft copolymers formed in a homogeneous blend of PS-mCOOH/poly(styrene-*ran*-glycidyl methacrylate) [PS–GMA] were compared with those formed in the heterogeneous blend of PS-mCOOH/PMMA–GMA.

For the homogeneous blend, the number of chains (n) of PS-mCOOH grafted onto a PS–GMA in in situ formed graft copolymers was ~4 although the maximum possible n is ~7. This is due to the steric hindrance by the already existing grafted chains. However, for the heterogeneous blends, n appeared not to be much affected by both f and the molecular weight of PMMA–GMA, and n was ~1 because of the existence of an interface between PS and PMMA phases in addition to the steric hindrance.

The weight fraction of graft copolymers in the blends, $w_{\text{copolymer}}(blend)$ was found to increase with f. However, the interfacial areal density of PMMA-*g*-PS was constant as ~0.02 chains/nm^2 regardless of f and the molecular weights of initially added PMMA–GMA. © 2001 Published by Elsevier Science Ltd.

Keywords: Reactive blend; Characterization of in situ graft copolymer; Interfacial activity

1. Introduction

Reactions at the interface in reactive blends produce copolymers with various structures depending upon the molecular structure of an initially added reactive compatibilizer. These in situ formed copolymers can be divided into three classes: block and graft copolymers, and crosslinked polymers. If both of the reactive species are end functional polymers, a block-type copolymer is formed at the interface [1–5]. Guégan et al. [1] studied the interfacial reaction kinetics of the immiscible blend of poly(methyl methacrylate) (PMMA) and polystyrene (PS) using epoxy terminal PMMA (PMMA-E) and carboxylic acid terminal PS (PS-COOH). By using narrow molecular weight distributions of PMMA-E and PS-COOH synthesized anionically, they could quantify, through size exclusion chromatography (SEC) — a powerful technique for the characterization of the in situ formed block copolymer — the conversion into block copolymer with mixing time. They also reported that PMMA-*g*-PS copolymer formed in situ from the reaction between PS-COOH and poly(methyl methacrylate-*ran*-glycidyl methacrylate) (PMMA-*r*E) with 35 epoxy functional groups has only single PS-COOH chain grafted onto PMMA-*r*E. Macosko and coworkers [2,3] reported that the reactivity of end functional groups affects considerably the morphology of the reactive blend. When a blend is prepared from constituent components with very fast reaction rate, it has the self-assembled morphology observed typically for the pre-made block copolymers due to the interface roughening and almost 100% conversion into the block copolymer [2,3].

When one of the in situ compatibilizers is an end functional polymer and the other has functional groups with more than two randomly distributed along a compatibilizer chain, graft copolymers are formed in situ at the interface. Many reactive blends produce graft copolymers since multi-functional compatibilizers are more available than end functional polymers [6–8]. However, there has seldom been research on the characterization of the graft copolymers formed in situ in reactive blends [9–14]. Furthermore, the in situ formed graft copolymer at the interface has been treated as the block copolymer neglecting its molecular structure [9–10]. Beck Tan et al. [9]used the solvent extraction method to quantify the

* Corresponding author. Tel.: +82-54-279-2276; fax: +82-54-279-8298.

[1] Present address: Department of Chemical Engineering and Material Science, University of Minnesota, 421 Washington Av. S.E., Minneapolis, MN 55455, USA.

E-mail address: jkkim@postech.ac.kr (Jin Kon Kim).

0032-3861/01/$ - see front matter © 2001 Published by Elsevier Science Ltd.
PII: S0032-3861(00)00543-7

amount of the polystyrene-*graft*-amorphous polyamide (PS-*g*-aPA) copolymer formed in situ in the poly(styrene-*co*-oxazoline) (PS-ox) and aPA blend. Assuming that a single aPA chain is grafted on a PS-ox chain and PS-*g*-aPA is regarded as the PS-*block*-aPA, they estimated the interfacial areal density, Σ of PS-*g*-aPA, of 0.04 chains/nm^2. Very recently, we found that 1.3–2 chains of poly(butylene terephthalate) (PBT) are grafted on a poly(styrene-*ran*-glycidyl methacrylate) (PS–GMA) chain in PBT/(PS + PS–GMA) blend using high temperature gel permeation chromatography [12]. Also the interfacial areal density was calculated to be 0.1 chains/nm^2 using the measured molecular weight of PS-*g*-PBT. Dedecker and Groeninckx [14] reported that the conformational restraints do not much affect the graft copolymer formation; thus, a very complex graft copolymer is formed in the blend of polyamide 6 and poly(styrene-*co*-maleic anhydride). The amount of the reacted anhydride groups was determined by FT-infrared spectra [13,14]. However, the quantitative characterization of the graft copolymers formed in situ in a reactive blend depending upon the amount of functional group has not been reported yet.

In this study, we characterized the graft copolymer formed in situ in the mono-carboxylated PS (PS-mCOOH) and poly(methyl methacrylate-*ran*-glycidylmethacrylate) (PMMA–GMA) blend using proton nuclear magnetic resonance spectroscopy (^{1}H-NMR) and GPC. Emphasis was placed on the difference between the graft copolymers formed in a PS-mCOOH/PMMA–GMA blend and a PS-mCOOH/PS–GMA blend, namely, the difference in graft copolymer formed between a heterogeneous blend and a homogeneous blend. Furthermore, graft copolymers formed in situ depending upon the molecular weight and the amount of GMA of PMMA–GMA were characterized. Here, we report the highlights of our findings.

2. Experimental section

2.1. Sample preparation

The molecular characteristics of the polymers employed in this study are listed in Table 1. PS–GMA for the homogeneous blend is a fractionated one from a PS–GMA [12] with a molecular weight distribution M_w/M_n of 2.5 using the solvent (toluene) and nonsolvent (methanol) method.

PMMA–GMAs were prepared by a free radical polymerization. The GMA concentration in PMMA–GMA was easily controlled by using different mole ratios of GMA monomer to MMA monomer added initially into a reactor since the reactivity ratios of GMA and MMA are 0.71 and 0.52, respectively [15]. The mole percent of GMA in a PMMA–GMA was determined by 500 MHz ^{1}H-NMR (DRX 500, Bruker) and this is expressed by the number (x) in PMMA–GMAx. H and L in PMMA–GMAs represent higher and lower molecular weights of PMMA–GMA, respectively. The number of reactive groups per chain (f) in Table 1 is calculated based on the molecular weight at peak of GPC chromatogram, M_p. PMMA–GMA8H was obtained by the fractionation of PMMA–GMA8L using the solvent/nonsolvent fractionation method. The solvent and the nonsolvent for PMMA–GMA were toluene and n-hexane, respectively.

All the polymers were dried under vacuum for more than 24 h at 70°C. The homogeneous blend of 90/10 (wt/wt) PS-mCOOH/PS–GMA was prepared in a MiniMax Molder at 220°C for 20 min under nitrogen atmosphere. The maximum shear rate was 20 s^{-1}, and the total blend weight was 1 g. Heterogeneous blends of 75/25 (wt/wt) PS-mCOOH/PMMA–GMA were prepared under the same conditions as the homogeneous blend. The solution-blended samples were prepared by dissolving PS-mCOOH and PMMA–GMA in toluene separately, and then mixing them, followed by precipitation into methanol. After drying for more than two days, the solution blended samples were sheared at 20 s^{-1} in the MiniMax molder at 220°C for 20 min. A Field emission scanning electron microscope (FESEM; S-4200, Hitachi) and a transmission electron microscope (TEM; JEOL 1200EX) were used to investigate the morphology of the blends. For SEM observation the PMMA–GMA phase was etched out by acetic acid to enhance the contrast of the cryogenically fractured surface; thus it looks dark in the SEM image. The Quantimet 570 image analyzer (Cambridge Instrument) was used to measure the surface area average diameter D_s of the dispersed phase. About 200–300 particles are employed to calculate D_s. The cross sectional area (A_i) of each particle on the micrograph was measured, and then converted to the diameter (D_i) of the circle having the same cross sectional area.

$$D_i = 2(A_i/\pi)^{1/2} \tag{1}$$

$$D_s = \frac{\sum_i D_i^3}{\sum_i D_i^2} \tag{2}$$

A very thin film with 70 nm thickness was prepared by slicing TEM specimens using a microtoming machine (MT-7000, Research and Manufacturing Company) with a diamond knife at room temperature. This thin film was stained for 15 min under ruthenium tetroxide (RuO_4) vapor. The PS phase appears dark due to selective staining.

2.2. Solvent extraction method

The unreacted PS-mCOOH in PS-mCOOH/PMMA–GMA blends was dissolved out from the blend using a solvent mixture of 80/20 v/v cyclohexane/toluene for four days at room temperature. The remains (namely, unreacted PMMA–GMA and PMMA-*g*-PS) were separated from the solution using an ultra-centrifuge (IECCENTRA-HN; IEC). Then they were dissolved into toluene, followed by

Table 1
Molecular characteristics of polymers used in this study

Polymer	M_n	M_p	M_w/M_n	Mole percent of GMA (mol%)	Number of functional groups per chain[a] (f)	η^* (Pa s) at $\omega = 20$ rad/s and 220°C
PS-mCOOH	89 000	167 000	1.50		1	640
PS–GMA	94 000	124 000	1.56	1.5	17.5	–[b]
PMMA–GMA0.7L	33 000	35 000	1.46	0.7	2.4	–[b]
PMMA–GMA8L	28 600	30 000	1.60	8.3	24.1	220
PMMA–GMA0.3H	53 000	87 000	1.79	0.3	2.6	1610
PMMA–GMA2H	53 000	63 000	1.55	2.0	12.5	1420
PMMA–GMA8H	71 000	80 000	1.19	8.3	64.2	–[b]

[a] Calculated values based on the molecular weight at peak, M_p.
[b] Not measured due to the limited amounts available.

precipitation of PMMA-*g*-PS and unreacted PMMA–GMA using a solvent mixture of 80/20 v/v cyclohexane/toluene for complete separation. The unreacted PS-mCOOH dissolved in the solvent mixture was precipitated using methanol. The 500 MHz ^{1}H-NMR was used to measure the amount of PMMA-*g*-PS formed in situ in the blend. We found that almost all PMMA-*g*-PS remained in the extracted PMMA phase from ^{1}H-NMR analysis; thus a very small amount of PMMA-*g*-PS (less than 0.5 wt%) in the extracted PS phase was neglected in the calculation of the weight fraction of PMMA-*g*-PS in total blend.

In order to measure the molecular weight of PMMA-*g*-PS, gel permeation chromatography (GPC; Waters 600E, Millipore) with UV detector was employed. By setting the wavelength to 260 nm, which is the characteristic wavelength of styrene, we determined the molecular weight of only PMMA-*g*-PS from the phase consisting of unreacted PMMA–GMA by using a calibration curve prepared with PS standards. This is because the PMMA does not give any UV signal in the above wavelength. We found that the molecular weight determined by using a calibration curve prepared with nine standard PMMAs is almost the same (at most 20% difference at a given retention volume) as that obtained from PS standards. For instance, a monodisperse PMMA with 420 000 and a monodisperse PS with 350 000 had the same retention volume of 18 ml in GPC, while a monodisperse PMMA with 18 000 and a monodisperse PS with 16 000 had the same retention volume of 21 ml in GPC. Thus, the molecular weight of PMMA–GMA calibrated by PS standards and not by PMMA standards was employed in the calculation of the number of grafted chains, n.

However, since the hydrodynamic volume for homopolymers (or PMMA-*block*-PS) might be different from that of PMMA-*g*-PS, the molecular weight of PMMA-*g*-PS determined by GPC with PS calibration curve might be different from the absolute molecular weight obtained with laser light scattering, even though it was reported that the difference in measured molecular weights by GPC with PS calibration curve between six-arm star-PS and linear PS with the same degrees of polymerization is less than 20% [16,17]. In order to test this argument, we removed the unreacted PMMA–GMA in the mixture of PMMA-*g*-PS and PMMA–GMA by dissolving it out using an acetic acid for four days at 60°C. Then PMMA-*g*-PS itself was separated from the solution using an ultracentrifuge at 8000 rpm. The absolute molecular weight of PMMA-*g*-PS was determined by GPC equipped with MALLS (Multi Angle Laser Light Scattering) (GPC-MALLS) at the Department of Chemistry in POSTECH, Korea, with measured value of dn/dc. The detectors in GPC-MALLS employed were a UV detector (UV 100, Spectra series), a RI detector (Optilab 903, Wyatt Technology), and a MALLS detector (Mini-Dawn, Wyatt Technology). The PMMA-*g*-PS solution in THF (0.2 wt% in solid) was injected at a rate of 0.8 cc/min. By using GPC-MALLS, the absolute values of the number-average and weight-average molecular weights (M_n and M_w), and the molecular weight at peak (M_p) in GPC-MALLS are simultaneously determined. As will be shown later, we found that the difference between the absolute molecular weight determined from GPC-MALLS and the molecular weight determined from GPC only with PS calibration curve was less than 20%. This small difference between two methods, namely the negligible effect of the hydrodynamic effect between PMMA-*g*-PS and PS (or PMMA and PS-*block*-PMMA), might be due to the fact that (i) the retention volume of PMMA is very similar to that of PS at the same molecular weight, as described already, and (ii) the n in PMMA-*g*-PS was found to be 1–2, as will be shown later; thus the chain conformation of PMMA-*g*-PS obtained in this study is not much different from PMMA-*block*-PS.

On the basis of the above arguments, in this study the value of n was calculated from the molecular weights of PMMA-*g*-PS, PS-mCOOH, and PMMA–GMA determined from the GPC chromatogram with PS standards as follows.

$$n = (M_{\text{PMMA-}g\text{-PS}} - M_{\text{PMMA–GMA}})/M_{\text{PS-mCOOH}} \quad (3)$$

Since PS-mCOOH and PMMA–GMA are polydisperse, PMMA-*g*-PS also shows polydispersity. Thus, the value of n changed depending on the different definitions for the

molecular weight. In this study, three different molecular weights are used: the peak molecular weight M_p, corresponding to a molecular weight at the peak in GPC chromatogram, M_n and M_w. The number of grafted chains calculated using Eq. (3) with M_n, M_p, and M_w is referred to as n_n, n_p and n_w, respectively.

2.3. ^{1}H-NMR analysis

The ^{1}H-NMR spectra of neat PS-mCOOH and PMMA–GMA are given in Fig. 1. Neat PS-mCOOH showed the peaks appearing at $\delta = 1.2$–2.3 ppm due to aliphatic hydrogens of the backbone and the peaks at $\delta = 6.3$–7.2 ppm from aromatic hydrogens (marked by **1**) of the phenyl ring. Also, it is seen in Fig. 1b that PMMA–GMA showed the characteristic peaks appearing at $\delta = 3.6$ ppm for the methoxy group in MMA (marked by **1**) and peaks appearing at $\delta = 3.8$–4.3, 3.2, and 2.6–2.8 ppm corresponding to hydrogens in GMA (marked by **2**, **3**, and **4**) [18]. The mole percent of GMA in a PMMA–GMA polymerized by a free radical polymerization was determined by the area of peak **3** divided by one-third of the area of peak **1** in the PMMA–GMA spectrum.

Fig. 2 gives the ^{1}H-NMR spectrum of the phase consisting of PMMA-*g*-PS and unreacted PMMA–GMA separated from 75/25 (wt/wt) PS-mCOOH/PMMA–GMA blend. Peak **2** at $\delta = 6.3$–7.2 ppm corresponding to the PS in the PMMA-*g*-PS is clearly seen in Fig. 2. We found that the phase of the blend undissolved by the solvent consisted of almost all the PMMA-*g*-PS and unreacted PMMA–GMA. This was because the characteristic peaks of PMMA–GMA could not be observed in the NMR spectrum of the dissolved phase of unreacted PS-mCOOH. Also, when the blend of PS-mCOOH and PMMA was extracted in the same way, the spectrum of each separated phase was exactly the same as that of neat PS-mCOOH or PMMA. Thus, we could neglect the possibility of a residue of the unreacted PS-mCOOH in the undissolved phase.

The molar ratios of MMA (x), GMA (y), and styrene (z) of the undissolved phase of the blend were determined as

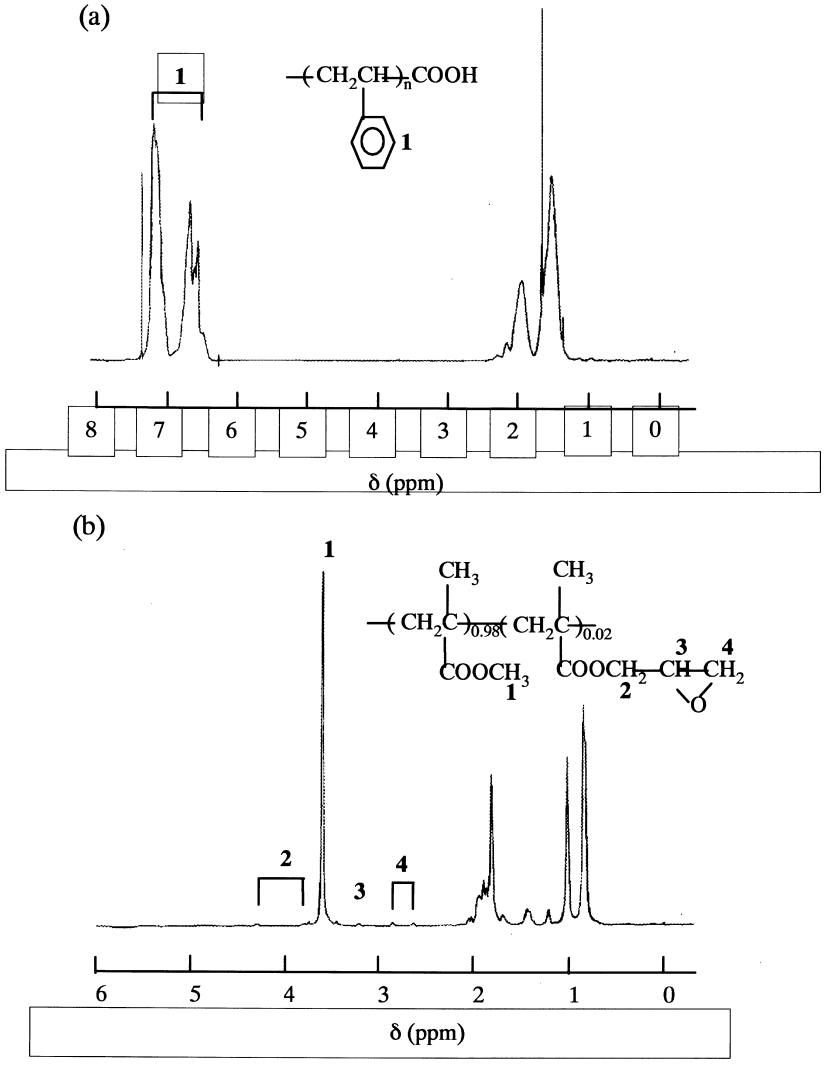

Fig. 1. ^{1}H-NMR spectra of (a) neat PS-mCOOH and (b) neat PMMA–GMA.

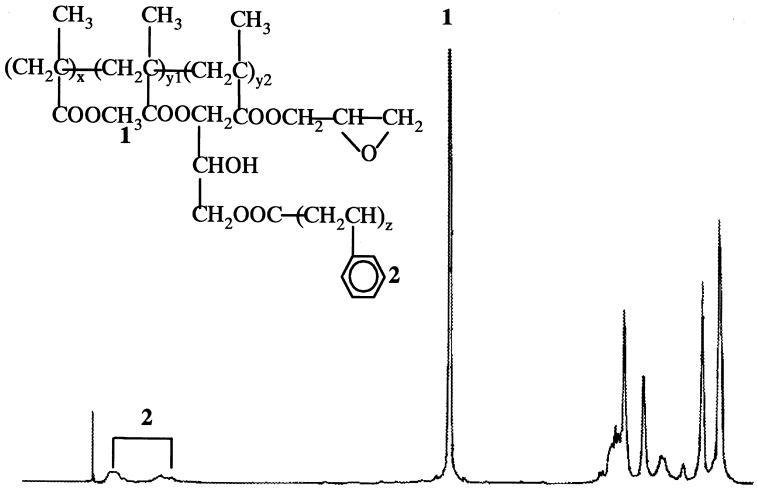

Fig. 2. ^{1}H-NMR spectrum of the PMMA–GMA phase separated from 75/25 (wt/wt) PS-mCOOH/PMMA–GMA2H blend.

follows. The z was easily determined by the area of peak **2** appearing at $\delta = 6.3$–7.2 ppm divided by 5. The mole fraction of MMA (x) was given by the amounts of MMA in unreacted PMMA–GMA as well as in the PMMA-g-PS; thus it was determined by the area of peak **1** appearing at $\delta = 3.6$ ppm divided by 3. Finally, the mole fraction of GMA (y) was expressed as x times $y_0/(1 - y_0)$, where y_0 is the mole fraction of GMA in initially added PMMA–GMA. This is because the mole fraction of GMA in PMMA–GMA does not change even if the PMMA-g-PS is formed through the opening of epoxy rings in GMA. Once the values of x, y and z are determined, the PS weight fraction in the undissolved phase consisting of PMMA–GMA and PMMA-g-PS, w_{PS}(extract) is given by

$$w_{PS}(\text{extract}) = \frac{zM_{0,s}}{(xM_{0,MMA} + yM_{0,GMA} + zM_{0,s})} \quad (4)$$

where $M_{0,i}$ is the molar mass of i monomer.

3. Results and discussion

3.1. Homogeneous blend

A homogeneous blend of 90/10 (wt/wt) PS-mCOOH/PS–GMA was prepared by melt blending in order to investigate the degree of grafting in the homogeneous state. The mole ratio of GMA to COOH in this blend, C_{GMA}/C_{COOH}, is 2.6 using the functionalities calculated based on the molecular weights at peak, M_p given in Table 1. This implies that the maximum possible number of grafted chains (n_{max}) of PS-mCOOH onto a PS–GMA is ~7 (namely, f_{GMA} in PS–GMA divided by 2.6) if all PS-mCOOH chains are assumed to be grafted uniformly on all PS–GMA chains.

Fig. 3 shows the GPC chromatograms of the PS-mCOOH, PS–GMA, and 90/10 (wt/wt) PS-mCOOH/PS–GMA blends. The peak position in the GPC chromatogram of the blend moved slightly to a shorter elution time, and a shoulder due to the reaction between PS-mCOOH and PS–GMA was clearly seen. The $M_{p,1}$ is 203k, corresponding to $n_p \sim 0.5$; thus this peak does not come from graft copolymer, but comes from the mixture of unreacted PS-mCOOH, unreacted PS–GMA, and part of the graft copolymers. A shoulder observed at a lower retention time is due to the graft polymers. If the chromatogram was separated roughly using the PeakFit program (PeakFit™ v.4.01, AISN Software Inc.), the molecular weight ($M_{p,2}$) corresponding to a shoulder in GPC chromatogram (marked by an arrow) is about 722k. This means that 3.6 chains of PS-mCOOH are, on average, grafted on a PS–GMA chain in the mixing time of 20 min at 220°C. Interestingly, in order to accommodate ~4 chains of PS-mCOOH per PS–GMA chain, the PS–GMA backbone chain of the graft polymer has to be stretched to a certain extent. If ~4 chains of PS-mCOOH are evenly grafted onto a PS–GMA, the molecular weight of PS–GMA between nearest neighbored grafted points is ~25k (= M_p/5). If PS-mCOOH chains are grafted in zigzag style onto a PS–GMA, the molecular weight of PS–GMA between nearest neighbor grafted points in one plane is ~50k. This zigzag style would be possible since graft copolymers are also polystyrene; thus, there is no energy penalty.

However, for heterogeneous blends discussed later, almost all grafted chains are directed towards the same direction to reduce the interfacial energy. Even if a zigzag style is considered, the molecular weight of graft PS-mCOOH chains is still three times larger than the molecular weight of PS–GMA (~50k) between nearest neighbor grafted points, because M_p of the grafted PS-mCOOH chain is 167k. Thus, both PS–GMA and PS-mCOOH should be stretched to have chain dimensions larger than their own R_g to reduce the steric hindrance by the already grafted chains. As the numbers of the PS-mCOOH grafted onto a PS–GMA chain increase, this barrier would be higher, implying that the higher degree of grafting does not seem

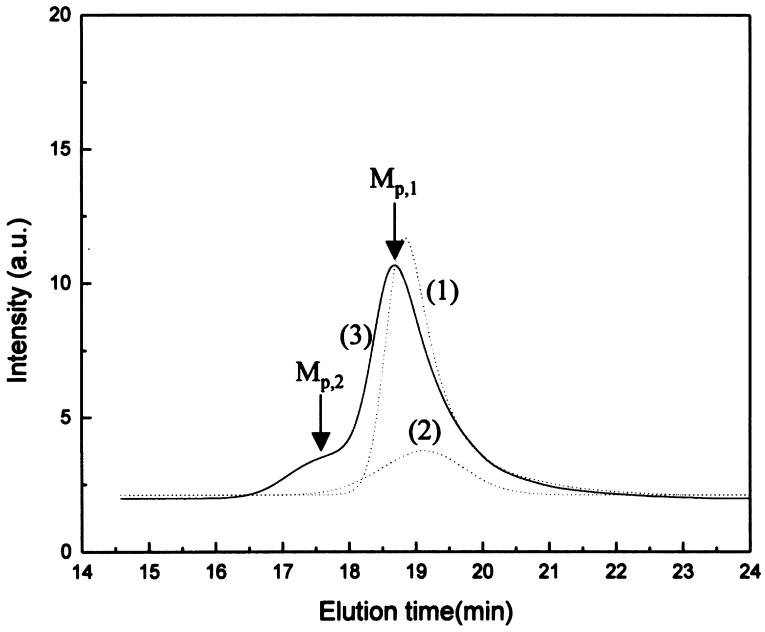

Fig. 3. GPC chromatograms for the homogeneous blend of 90/10 (wt/wt) PS-mCOOH /PS–GMA with $C_{GMA}/C_{COOH} = 2.6$: (1) PS-mCOOH, (2) PS–GMA, and (3) PS-mCOOH /PS–GMA blend. The molecular weights at peak of the graft polymers are marked by an arrow.

to be attained even though many functional groups are still available in a PS–GMA chain. Therefore, we concluded that the steric effect is very important to determine *n* and that this effect would be much stronger in the heterogeneous case due to the existence of a finite interface.

3.2. Heterogeneous blends

Fig. 4a shows the GPC chromatograms of (1) unreacted PMMA–GMA8L, (2) unreacted PS-mCOOH, and (3) the mixture of PMMA-*g*-PS copolymers and unreacted PMMA–GMA8L, which was extracted from the blends of PS-mCOOH/PMMA–GMA8L. Curve (1) was obtained using an RI detector, and curves (2) and (3) using a UV detector. Since PMMA cannot be detected from a UV detector, the curve (3) essentially represents the PMMA-*g*-PS copolymer itself. In Fig. 4a, two GPC chromatograms are added: curve (4), obtained by using the RI detector for the mixture of PMMA-*g*-PS, and unreacted PMMA–GMA8L, which is the same material as employed in curve (3), and curve (5) by using the RI detector for PMMA-*g*-PS itself, namely free of unreacted PMMA–GMA8L. Comparing curve (5) with curve (4) in Fig. 4a, we found that PMMA-*g*-PS itself does not contain any unreacted PMMA–GMA8L, because curve (5) does not have any GPC chromatogram corresponding to PMMA–GMA8L. Furthermore, as expected, the curves (3) and (5) are essentially the same; thus in order to obtain the GPC chromatogram for PMMA-*g*-PS itself, we did not need to remove the unreacted PMMA–GMAs in the mixture of PMMA-*g*-PS and PMMA–GMAx, once the UV detector was used. Fig. 4b gives the GPC chromatograms of (1) unreacted PMMA–GMA0.7L using the RI detector, (2) unreacted PS-mCOOH, and (3) the mixture of PMMA-*g*-PS copolymers and unreacted PMMA–GMA0.7L using the UV detector.

It is seen from Fig. 4a and b that the elution times

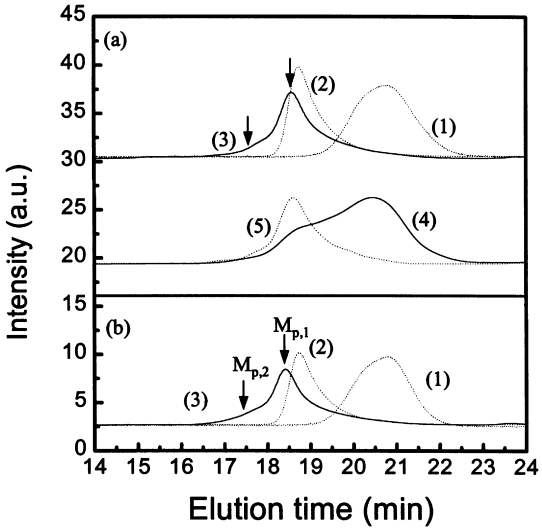

Fig. 4. GPC chromatograms of (1) unreacted PMMA–GMAL, (2) unreacted PS-mCOOH and (3) PMMA-*g*-PS extracted from the blends of 75/25 (wt/wt) PS-mCOOH/PMMA–GMAL: (a) 8 mol% and (b) 0.7 mol% of GMA. Curve (1) was obtained using the RI detector, whereas curves (2) and (3) using the UV detector. Two additional curves are added to Fig. 4a: (4) the mixture of PMMA-*g*-PS and unreacted PMMA–GMA8L using the RI detector and (5) PMMA-*g*-PS itself using the RI detector. We found that the GPC chromatogram using the UV detector was essentially the same as the curve (5). The arrows indicate two peaks obtained by the separation of the GPC chromatogram of PMMA-*g*-PS.

corresponding to PMMA-*g*-PSs are shorter than those corresponding to unreacted PMMA–GMA and unreacted PS-mCOOH. This implies that PMMA-*g*-PS was formed in situ by the reaction between the epoxy group in PMMA–GMA and the carboxylic acid in PS-mCOOH. Table 2 gives the values of M_p, M_n, M_w, n_p, n_n, and n_w of all in situ formed copolymers determined by the PS standard calibration curve. At this point, we discuss the validity of M_w measured by the GPC chromatogram given in curve (3) or curve (5) of Fig. 4a. For this purpose, PMMA-*g*-PS itself prepared by PS-mCOOH and PMMA–GMA8L was successfully separated from all components in the blend, as shown in curve (5) in Fig. 4a. Using GPC-MALLS with the measured value of $dn/dc = 0.155$ cc/*g* the M_p and M_w of PMMA-*g*-PS itself were determined to be 215 000 and 255 000. Since the M_p and M_w calculated from GPC only with PS standards were 209 000 and 251 000 (see Table 2), the difference between the two methods (GPC with PS calibration and GPC-MALLS) is less than 10%. Therefore, we conclude that the molecular weight of PMMA-*g*-PS obtained from GPC only with PS calibration was quite reasonable. Also, using 500 MHz ^{1}H NMR, the mole fraction of PS in the PMMA-*g*-PS itself prepared by PS-mCOOH and PMMA–GMA8L was determined to be 0.72. Because the mole fraction is related to the M_n, the value of n_n (the number of the graft chain on the basis of M_n) was determined to 0.83, which is close to n_n obtained from GPC only with PS calibration (see Table 2).

Interestingly, the M_ps of all PMMA-*g*-PSs were approximately the sum of those of unreacted PS-mCOOH and corresponding PMMA–GMA and appeared not to be affected by the mole percent of GMA (or, functionality *f*). These results were considered to be reasonable compared with n_p in the homogeneous blend where the n_p was ~4. If the molecular weight between nearest neighbor PS-mCOOH chains grafted on a PMMA–GMA chain is two times larger than that on a PS–GMA due to the existence of the interface between PS and PMMA phases, this value is ~50k. This value is larger than the M_ps of the L-series of PMMA–GMA (see Table 1). Therefore, when a similar steric effect as in the homogeneous blend is assumed, n_p would be ~1. However, n_w was ~2 regardless of *f* of PMMA–GMA. Generally, M_w is higher than M_p for polydisperse polymers like PMMA–GMA and PMMA-*g*-PS employed in this study, but the PS-mCOOH used in this study shows the asymmetric GPC chromatogram resulted in lower M_w than M_p. Consequently n_w is calculated to be higher than that based on M_p. It is also seen in Fig. 4 that there exist higher molecular weights of PMMA-*g*-PS corresponding to a tail located at a shorter elution time (~17.7 min) in addition to the main peak position. As discussed in detail later, this might be attributed to the reaction of PS-mCOOH and the higher molecular weight portion of the L-series of PMMA–GMAL.

The molecular weight effect of PMMA–GMA was investigated using the H-series of PMMA–GMA*x* (x = 0.3, 2, and 8) with M_p two to three times higher than that of the L-series of PMMA–GMA. The GPC chromatograms of PMMA-*g*-PS, unreacted PS-mCOOH and unreacted PMMA–GMA*x*H of a 75/25 (wt/wt) PS-mCOOH/PMMA–GMAxH blend are given in Fig. 5, and the M_p, M_w, n_p, and n_w of PMMA-*g*-PS formed in situ in the blends are also listed in Table 2. Again, using GPC-MALLS with the measured value of $dn/dc = 0.144$ cc/*g*, the M_p and M_w of PMMA-*g*-PS itself prepared by PS-mCOOH and PMMA–GMA2H were determined to be 230 000 and 430 000. Since the M_p and M_w calculated from GPC only were 227 000 and 424 000 (see Table 2), the difference between the two methods (GPC with PS calibration and GPC-MALLS) is less than 10%. Also, using 500 MHz ^{1}H NMR, the mole fraction of PS in the PMMA-*g*-PS itself was determined to be 0.60, from which we estimated the $n_n = 0.9$, which is close to n_n obtained from GPC only with PS calibration (see Table 2).

Similar to the results for the blends with the L-series of PMMA–GMA, the GPC chromatograms of PMMA-*g*-PS are very similar to each other regardless of *f* of the PMMA–GMAH chain, and n_p is ~1. If we consider the existence of the interface and the steric hindrance due to the grafted chains as in the homogeneous blend, i.e. PS-mCOOH chains are assumed to be grafted on a PMMA–GMAH chain with the molecular weight between graft points of ~50k, n_p would be 1.2–1.5. This means that the interface in the heterogeneous blend is another barrier against the grafting reaction of PS-mCOOH on PMMA–GMA as well as the steric hindrance by already grafted chains. However, compared with results given in Fig. 4, as the molecular weight of PMMA–GMA increases, the higher molecular weight portion corresponding to a shorter

Table 2
Molecular weights and number of grafting of PMMA-*g*-PS formed in situ in 75/25 (wt/wt) PS-mCOOH/PMMA–GMA blends

	PMMA–GMAL		PMMA–GMAH		
mol% of GMA	0.7	8	0.3	2	8
M_p	245 000	209 000	233 000	227 000	262 000
n_p	1.2	1.1	0.9	1.0	1.1
M_w	289 000	251 000	404 000	424 000	472 000
n_w	1.8	1.5	2.3	2.6	2.9
M_n	121 000	97 000	120 000	167 000	210 000
n_n	1.0	0.8	0.8	1.3	1.6

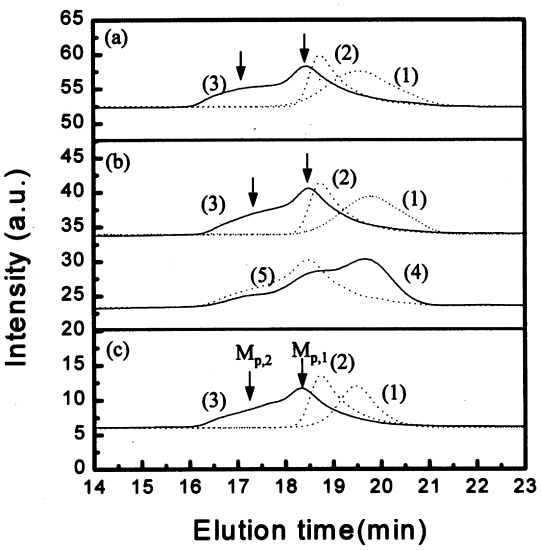

Fig. 5. GPC chromatograms of (1) unreacted PMMA–GMAH, (2) unreacted PS-mCOOH and (3) PMMA-*g*-PS extracted from the blends of 75/25 (wt/wt) PS-mCOOH/PMMA–GMAH: (a) 0.3 mol%, (b) 2 mol%, and (c) 8 mol% of GMA. Curve (1) was obtained using the RI detector, curves (2) and (3) using the UV detector. Two additional curves are added to Fig. 5b: (4) the mixture of PMMA-*g*-PS and unreacted PMMA–GMA2H using the RI detector and (5) PMMA-*g*-PS itself using the RI detector. We found that the GPC chromatogram using the UV detector was essentially the same as the curve (5). The arrows indicate two peaks obtained by the peak separation of GPC chromatogram.

elution time increases, although the major number of grafted chains, n_p, is ~1 regardless of the molecular weight and f of the PMMA–GMA. Thus when n_w for the blends with the H-series of PMMA–GMA is calculated instead of n_p, it is ~3, larger than that (~2) for the blends with the L-series of PMMA–GMAL.

It is seen from Figs. 4 and 5 that when the GPC chromatogram of PMMA-*g*-PS in the blends was separated into two peaks using the PeakFit™, the ratio (R_{A2}) of the area of peak 2 ($A_{p,2}$) corresponding to higher molecular weights to the total area ($A_{p,1} + A_{p,2}$) in the GPC chromatogram for blends with the H-series of PMMA–GMA is much larger than that for blends with the L-series of PMMA–GMA. Also, the peak molecular weight ($M_{p,2}$) marked by the arrow in Fig. 5 corresponding to blends with the H-series of PMMA–GMA is larger than that in Fig. 4 corresponding to the blends with the L-series of PMMA–GMA. These different behavior can be attributed to the larger amount of the higher molecular weight portion of the H-series of PMMA–GMA compared with the L-series of PMMA–GMA, since the average molecular weight of PMMA–GMAH is 2–3 times larger than that of PMMA–GMAL (see Table 1).

Let us first consider a blend with PMMA–GMA0.3H as shown in Fig. 5, where $M_{p,2} \sim 1000$k, $M_{p,1} \sim 233$k and $R_{A2} \sim 0.3$. In this situation, one attempts to calculate the weight fraction ($W_{PMMA-GMA}(MW)$) of PMMA–GMA with a certain MW in the intially added PMMA–GMA and the molecular weight (MW) of PMMA–GMA that is employed in $M_{p,2}$ of PMMA-*g*-PS. The $W_{PMMA-GMA}$ (MW) with a certain MW employed in the formation of 1000k PMMA-*g*-PS is simply calculated as:

$$W_{PMMA-GMA}(MW) = R_{A2} \times w_{copolymer}(blend) \times (MW/1000k)/w_{PMMA-GMA} \quad (5)$$

Here, $w_{PMMA-GMA}$ is the weight fraction of PMMA-GMA in the blend (0.25) and $w_{copolymer}(blend)$ is the weight fraction of total PMMA-*g*-PS formed in situ in the blend, which will be determined later (see Table 3). Notice that MW in Eq. (5) depends upon n since MW is given by $1000k - nM_{p,PS-mCOOH}$ (see Eq. (3)). If we assume that n is roughly estimated from the MW/50k as described in the above, MW of PMMA–GMA0.3H would be 230k and $n \sim 5$. The value of $n \sim 5$ is not exaggerated, since n_w corresponding to the weight average molecular weight was ~3 (see Table 2) and PMMA–GMA chains with MW of ~230k have seven GMA groups per chain. On the basis of these values, we found that less than 0.5 wt% of PMMA–GMA0.3H with the MW of 230k gives about ~30% of higher peak areas in GPC chromatogram of PMMA-*g*-PS. From the GPC chromatogram of PMMA–GMA0.3H, we could measure the weight fraction of MW greater than 230k in the H-series PMMA–GMA to be at least 0.03.

Furthermore, even if $R_{A2} \sim 0.3$, the mole fraction (y) of PMMA-*g*-PS with 1000k in total PMMA-*g*-PS blend is just 0.09 using the following relationship:

$$\frac{(1000k)y}{(1000k)y + (233k)(1-y)} = R_{A,2} \quad (6)$$

This suggests that when the number of chains is considered instead of the weight, there exist only ~9 PMMA-*g*-PS chains with 1000k per 100 chains of PMMA-*g*-PS at the interface. Therefore, we concluded that most of the PMMA-*g*-PS chains (more than 90% of chains located at the interface) have only single grafted chain of PS-mCOOH.

For the blends with PMMA–GMA0.7L, $M_{p,2} \sim 460$k, $M_{p,1} \sim 245$k, and $R_{A2} \sim 0.10$. Following the above

Table 3
The copolymer weight fraction in the blend $w_{copolymer}(blend)$ and the interfacial areal density Σ of the graft copolymers formed in situ in the 75/25 (wt/wt) PS-mCOOH/PMMA–GMA

	PMMA–GMAL		PMMA–GMAH		
Mole% of GMA	0.7	8	0.3	2	8
D_s (μm)	0.77	0.23	0.73	0.32	0.26
w_{PS} (extract) (wt%)	6.4	13.9	3.9	9.5	18.6
$w_{copolymer}$ (*blend*)(wt%)[a]	1.8	4.0	1.4	3.2	6.1
Σ (chain/nm^2)[a]	0.024	0.019	0.018	0.019	0.025
δ (nm)	10	6.6	7.3	7.4	11.4

[a] Calculated values based on M_p.

argument, we found that less than 0.2 wt% of the PMMA–GMA0.7L with the MW of ~120k and $n \sim 2$ could contribute the tail of the higher molecular weight of PMMA-*g*-PS in the GPC chromatogram. Furthermore, y defined by Eq. (6) was calculated to be 0.05, implying that more than 95% of PMMA-*g*-PS chains located at the interface have only single grafted chain of PS-mCOOH.

Then, why is PMMA-*g*-PS with high n formed during melt blending of reactive blends? It might be related to morphological development during the blend. Thus, if morphological development is different, the value of n changes. To test this speculation, we prepared the 75/25 (wt/wt) PS-mCOOH/PMMA–GMA8H by solution blending using a cosolvent of toluene, followed by precipitation into methanol. Then, the powder forms of the blends were mixed in a Mini-Max molder at 220°C for 20 min. Fig. 6 shows the GPC chromatograms of PMMA-*g*-PS and unreacted polymers for the solution-blended sample. Comparing the chromatogram of Fig. 5c with that of Fig. 6, the higher molecular weight portion of PMMA-*g*-PS at a retention time of 17 min is much reduced for the solution-blended sample.

For a melt-blended sample, two phases with very large sizes (say pellet size) become a lace form at a short mixing time. In this case, some of the dispersed phases are extremely elongated at certain regions and the interfacial area per unit volume of PMMA–GMA becomes very large. Therefore, each chain of PMMA–GMA located at these regions should be highly stretched, implying that the area occupied by one PMMA–GMA chain would be very large compared with that at other regions. But the concentration of PS-mCOOH near the interface is similar to that in the bulk phase. Therefore, in these regions PMMA–GMA can accommodate more chains (say n is 3–4) of PS-mCOOH. However, since the interface area per unit volume of PMMA–GMA at other places is not large, PMMA–GMA is not strongly stretched. In this case, PMMA–GMA chains do not accommodate many chains of PS-mCOOH. If these speculations are reasonable, dispersed domains with very small size (similar to that of a micelle) are easily found for a melt-blended sample compared with a solution-blended sample.

Meanwhile, a solution-blended sample exhibited co-continuous structure. This is because a rapid precipitation is similar to a deep quenching into a spinodal decomposition. Previously, Lee and Han [19] also reported that three compositions (70/30; 50/50 and 30/70 wt/wt PS/PMMA) exhibited a co-continuous structure resulting from a spinodal decomposition even though the viscosity ratios differed from 1000 to 0.1. During a melt mixing of a solution-blended sample, the co-continuous structure in 75/25 (wt/wt) PS-mCOOH/PMMA–GMA was rapidly changed into dispersed domains. Therefore, there is little chance to find some regions having a very large interface where PMMA–GMA chains are highly stretched. Thus, the reaction occurs only at the interface covering the dispersed domains. In this case, when graft copolymers with $n_p \sim 1$ already cover the dispersed domains, it is very difficult for fresh PS-mCOOH existing far from the interface to reach the interface.

In order to test the above argument, TEM micrographs of

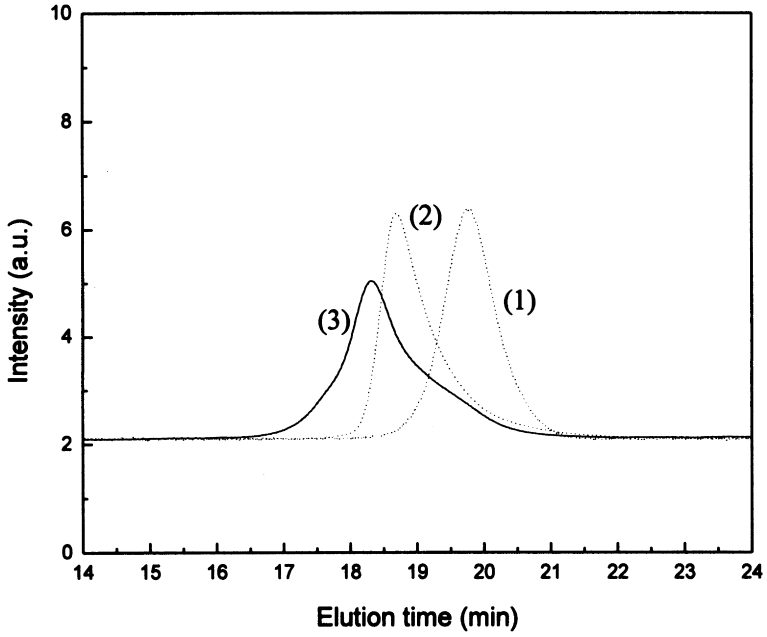

Fig. 6. GPC chromatograms of (1) unreacted PMMA–GMA8H, (2) unreacted PS-mCOOH, and (3) PMMA-*g*-PS extracted from the blends of 75/25 (wt/wt) PS-mCOOH/ PMMA–GMA8H prepared by solution blending followed by melt shearing at 20 s^{-1} for 20 min. Curve (1) was obtained using the RI detector, curves (2) and (3) using the UV detector.

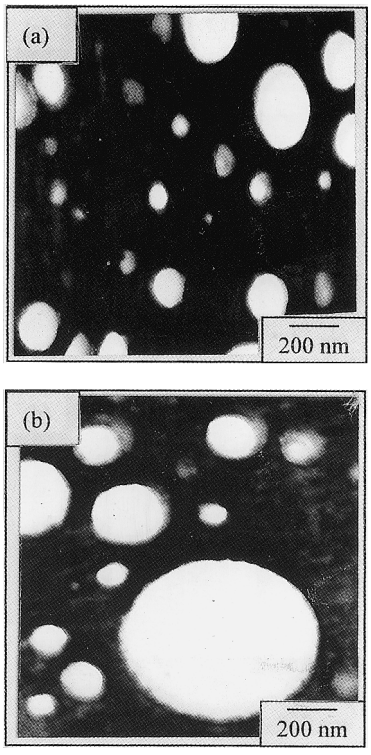

Fig. 7. TEM micrographs of 75/25 (wt/wt) PS-mCOOH/PMMA–GMA8H blends prepared by (a) melt blending and (b) solution blending followed by a melt shearing at 20 s^{-1} for 20 min.

melt-blended sample and solution-blended sample after melt mixing are shown in Fig. 7. It is seen that very small size dispersed domains (~20 nm) are clearly visible for a melt-blended sample compared with a solution-blended sample. Interestingly, the dispersed domain size of the former is smaller than that of the latter, which is different from the PBT/PS with PS–GMA [20]. This is because a solution-blended sample has co-continuous structures before a mixing resulting from a spinodal decomposition. But for 75/25 (wt/wt) PBT/PS blend, initial morphology after solution blending followed by precipitation has very fine and dispersed domains.

From the measured $w_{PS}(extract)$ using ^{1}H-NMR spectra and Eq. (4) and the MW and n_p of the PMMA-*g*-PS measured by GPC analysis, $w_{copolymer}(blend)$ and the interfacial areal density Σ could be obtained (Table 3):

$$w_{copolymer}(blend) = \frac{w_{PS}(extract) w_{PMMA\text{-}GMA} M_{copolymer}}{n M_{PS\text{-}mCOOH}} \quad (7)$$

$$\Sigma = \frac{w_{copolymer}(blend) N_{av} \rho_{blend} D}{6 M_{copolymer} \phi_d} \quad (8)$$

where $w_{PMMA\text{-}GMA}$ is the weight fraction of PMMA–GMA in the blend, N_{av} is Avogadro's number, ρ_{blend} is the density of the blend, D is the diameter of the dispersed domain, and ϕ_d is the volume fraction of the dispersed phase. ρ_{blend} is calculated using a mixing rule, $\rho_{blend} = w_{PS}\rho_{PS} + w_{PMMA}\rho_{PMMA}$, where w_{PS} is the weight fraction of PS, and ρ_{PS} and ρ_{PMMA} at 220°C are 0.96 [21] and 1.06 g/cc,[2] respectively.

The values of D for all blends are determined from Eqs. (1) and (2) and SEM micrographs given in Fig. 8. As shown in Fig. 8, with increasing f (or mole fraction) at a given M_w, the dispersed domain size decreased and the interfacial adhesion between the matrix and the domain became stronger; thus, the amount of graft copolymer increased.

The Σ and $w_{copolymer}$ (*blend*) in Table 3 were calculated based on the M_p. The Σ for the blends employed in this study appears to be nearly constant as ~0.02 chain/nm^2 irrespective of f and the molecular weight of PMMA–GMA. Recently, Rieman et al. [23] reported that the interfacial area occupied by a pre-made PS-*block*-PMMA, i.e. $1/\Sigma$, is larger than that (~10 nm^2/chain) occupied by a PS-*block*-PMMA chain forming micelles when PS-*block*-PMMA is used as a compatibilizer for PS/PMMA blend. In addition, their results showed that Σ ranged from 0.02 to 0.03 chain/nm^2 for the PS/PMMA blends with the PS-*block*-PMMA larger than 1 wt%. Therefore, the measured value of Σ (as ~0.02 chain/nm^2) seems to be reasonable. The $w_{copolymer}(blend)$ increases with f because of the faster reaction rate [24]. Faster reaction rate can stabilize the fine morphology by preventing the coalescence of the dispersed phase, i.e. resulting in higher $w_{copolymer}(blend)$ and smaller D_s.

Now, consider the thickness (δ) of graft copolymer layer using $w_{copolymer}(blend)$ with the assumption that $\rho_{blend} \sim \rho_{copolymer}$ and $D \gg \delta$,

$$\delta \cong \frac{w_{copolymer}(blend) D}{6\phi_{PMMA\text{–}GMA}} \quad (9)$$

As shown in Table 3, δ for the PS-mCOOH/PMMA–GMA blend is similar to the R_g (~10 nm) of PS-mCOOH. This indicates that the grafted PS chains are not much stretched. This is due to a relatively small interaction parameter χ (0.027) at 220°C for PMMA/PS blend [25]. Since the interface with a small χ can be stabilized easily by small amounts of graft copolymers, the interfacial reaction would not continue to make more graft copolymers against the barrier of the grafted layer. However, for a blend with a large χ (~0.1 for PS/poly(2-vinylpyridine) blend), the grafted layer was stretched to a value of 1.8–2 times R_g [26], in order to reduce the interfacial energy and to stabilize the interface by getting more fresh reactant polymers. This large stretch was also reported previously for PBT/(PS + PS–GMA) blend with χ of 0.156, in which Σ is ~0.1 chains/nm^2 and δ is ~11 nm corresponding to ~1.9$R_{g,PBT}$ [12]. However, very recently, Schulze et al. [27] reported that the molecular weight (M) of an end-functional polymer profoundly affected the value of Σ of a block (or graft) copolymer formed in situ in a reactive blend, for instance the larger M is, the smaller Σ is. Thus, the

[2] We calculated ρ_{PMMA} at 220°C using ρ_{PMMA} at T_g and the thermal expansion coefficient, $(1/V)(dV/dT)$ above T_g. $\rho_{PMMA}(T_g)$ is 1.15 g/cm^3, and $(1/V)(dV/dT)$ above T_g is 5.8×10^{-4} K^{-1}[22].

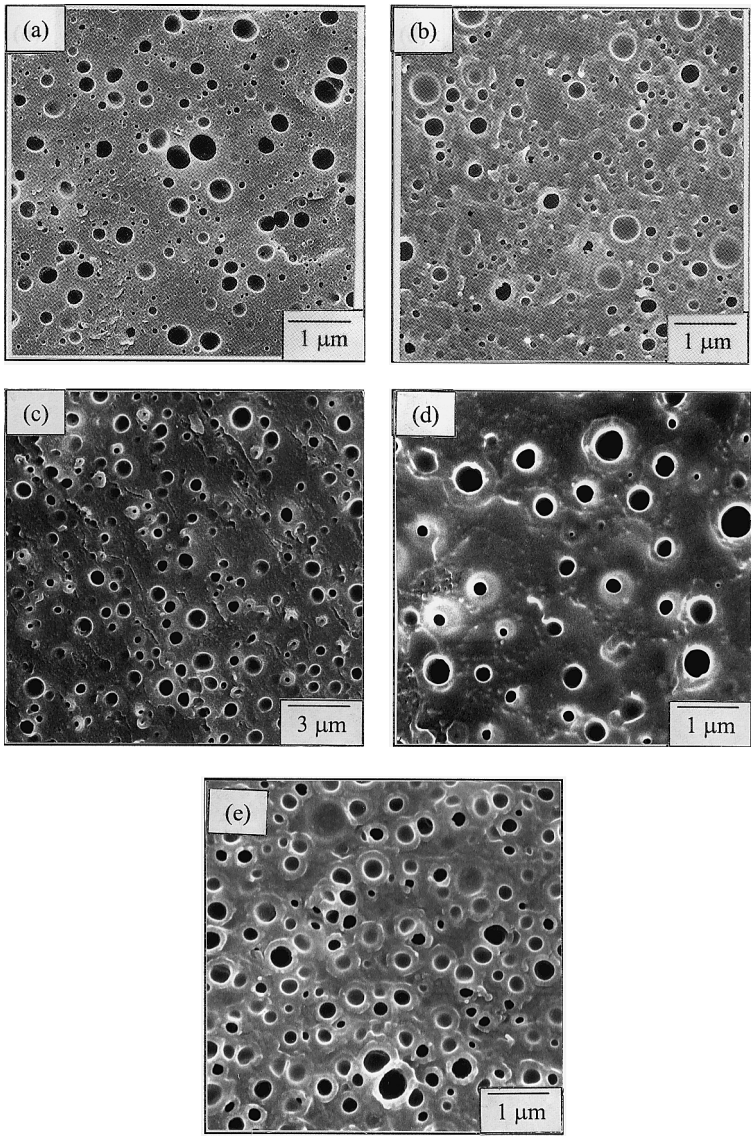

Fig. 8. SEM micrographs of 75/25 (wt/wt) PS-mCOOH/PMMA–GMAs blends:(a) PMMA–GMA0.7L; (b) PMMA–GMA8L; (c) PMMA-0.3H; (d) PMMA-2H; and (e) PMMA-8H.

difference in Σ between PS-mCOOH/PMMA–GMA blend and PBT/PS–GMA blend might be due to the fact that the $M_{\text{PS-mCOOH}}$ is 2–5 times larger than $M_{\text{PMMA}-\text{GMAs}}$ in this blend (see Table 1), whereas M_{PBT} is about half that of $M_{\text{PS}-\text{GMA}}$ in PBT/PS–GMA blend [12].

4. Conclusions

We have shown in this study that the graft copolymers formed in situ in the 75/25 (wt/wt) PS-mCOOH/PMMA–GMA blend depending upon the molecular weight and f of PMMA–GMA, were successfully characterized using ^{1}H-NMR and GPC. The graft copolymers formed in a homogeneous blend consisting of PS-mCOOH/PS–GMA were compared with those formed in the PS-mCOOH/PMMA–GMA blend.

For the homogeneous blend of 90/10 (wt/wt) PS-mCOOH/PS–GMA, the number of chains (n) of PS-mCOOH grafted onto a PS–GMA in in situ formed graft polymers was ~4, although the maximum possible n is ~7. This is due to the steric hindrance by the already existing grafted chains. However, for the heterogeneous blends, n did not appear to be much affected by both f and the molecular weight of PMMA–GMA, and n was ~1. This is because, in addition to the steric hindrance, the interface between two immiscible phases of PMMA and PS becomes another barrier against the interfacial grafting reaction.

The $w_{\text{copolymer}}(blend)$ determined from the ^{1}H-NMR and GPC was found to increase with f. However, Σ of PMMA-g-PS was constant (~0.02 chains/nm^2) regardless of f and the molecular weights of initially added PMMA–GMA. A rather small value is due to a smaller χ between PMMA and PS, since for a larger χ

such as found in PBT/PS, Σ of PS-*g*-PBT was increased to $\sim$0.1 chains/nm^2. The other possible reason is the relatively high molecular weight of PMMA-g-PS copolymers formed in situ in the blends.

Acknowledgements

We acknowledge that Prof. T. Chang at POSTECH kindly measured the absolute molecular weights of PMMA-*g*-PS using GPC-MALLS and that Professors C. Macosko in University of Minnesota and K. Char in Seoul National University read critically this manuscript. This work was supported by the Korea Research Foundation (1998-001-e01369) and POSTECH fund for Research Instrument (1999).

References

[1] Guégan P, Macosko CW, Ishizone T, Hirao A, Nakahama S. Macromolecules 1994;27:4993.
[2] Orr CA, Adedeji A, Hirao A, Bates FS, Macosko CW. Macromolecules 1997;30:1243.
[3] Lyu SP, Cernohous JJ, Bates FS, Macosko CW. Macromolecules 1999;32:106.
[4] Fleischer CA, Morales AR, Koberstein JT. Macromolecules 1994;27:379.
[5] Ibuki J, Charoensirisomboon P, Chiba T, Ougizawa T, Inoue T, Weber M, Koch E. Polymer 1999;40:647.
[6] Brown SB. In: Xanthos M, editor. Reactive extrusion — principles and practice. New York: Hanser, 1992 (chap. 4).
[7] Xanthos M, Dagli SS. Polym Engng Sci 1991;31:929.
[8] Liu NC, Baker WE. Adv Polym Tech 1992;11:249.
[9] Tan NCB, Tai SK, Briber RM. Polymer 1996;37:3509.
[10] Hu GH, Kadri I. J Polym Sci: Polym Phys Ed 1998;36:2153.
[11] Weber M, Heckmann W. Polym Bull 1998;40:227.
[12] Jeon HK, Kim JK. Macromolecules 1998;32:9273.
[13] Dedecker K, Groeninckx G. Macromolecules 1999;32:2472.
[14] Dedecker K, Groeninckx G, Inoue T. Polymer 1998;39:5001.
[15] Brosse J, Gauthier J. Lenain Makromol Chem 1983;184:505.
[16] Lee HC, Chang TH, Harville S, Mays JW. Macromolecules 1998;31:690.
[17] Lee HC, Lee W, Chang TH, Yoon JS, Frater DJ, Mays JW. Macromolecules 1998;31:4114.
[18] Zhang H, Ruckenstein E. Macromolecules 1998;31:4753.
[19] Lee JK, Han CD. Polymer 1999;40:2521.
[20] Jeon HK, Kim JK. Polymer 1998;39:6227.
[21] Richardson MJ, Savill NG. Polymer 1977;18:3.
[22] Brandrup J, Immergut EH, editors. 3rd ed. Polymer handbook, V-77. New York: Wiley-Interscience, 1989.
[23] Riemann RE, Cantow HJ, Friedrich Chr. Macromolecules 1997;30:5476.
[24] Jeon HK, Kim JK. Macromolecules 2000 (in press).
[25] Callaghan TA, Paul DR. Macromolecules 1993;26:2439.
[26] Dai KH, Kramer EJ. J Polym Sci: Polym Phys Ed 1994;32:1943.
[27] Schulze JS, Cernohous JJ, Hirao A, Lodge TP, Macosko CW. Macromolecules 2000;33:1191.